BIOCHEMISTRY
including biophysical chemistry & molecular biology
Article

Biochemistry **2009,** *48,* 7817–7823 7817
DOI: 10.1021/bi9006786

General Peroxidase Activity of G-Quadruplex−Hemin Complexes and Its Application in Ligand Screening[†]

Xiaohong Cheng,[‡,§] Xiangjun Liu,[‡] Tao Bing,[‡,§] Zehui Cao,[‡] and Dihua Shangguan*[,‡]

[‡]*Beijing National Laboratory for Molecular Sciences, Institute of Chemistry, Chinese Academy of Sciences, Beijing 100190, China, and* [§]*Graduate School of the Chinese Academy of Sciences, Beijing 100039, China*

Received April 21, 2009; Revised Manuscript Received June 19, 2009

ABSTRACT: DNA sequences with repetitive G-rich structural motifs, which form special structures called G-quadruplexes, widely exist in the human genome. Here we report the general peroxidase activity of G-quadruplex−hemin complexes and discuss the connection between peroxidase activity and G-quadruplex structures. The high peroxidase activity of hemin complexed with intramolecular parallel G-quadruplex-forming sequences in gene promoters (such as c-Myc, VEGF, c-Kit21, HIF-1α, and RET) may imply a potential mechanism of hemin-mediated cellular injury. This peroxidase activity has also been demonstrated to be applicable for screening G-quadruplex ligands (potential anticancer reagents) using colorimetric and visual detection strategies.

DNA and RNA sequences with repetitive G-rich structural motifs can fold into G-quadruplex structures, which are composed of stacked guanine tetrads (*1*). Interest in this structure has intensified in recent years because of its involvement in many important biological processes and its applications in supramolecular chemistry and nanotechnology (*2*). Genome-wide bioinformatic searches have revealed that 376000 potential G-quadruplex-forming sequences exist in the human genome (*3*, *4*), more than 40% of human gene promoters contain one or more quadruplex motifs (*5*), and these sequences are less common in tumor suppressor genes but highly present in proto-oncogenes (*6*). Evidence of the presence of the G-quadruplex motifs in vivo is accumulating, with them being found in c-Myc[1] (*7*), VEGF (*8*), c-Kit (*9*), HIF-1α (*10*), RET (*11*), and Bcl-2 (*12*) gene promoters, as well as in telomeres (*13*). G-Quadruplexes are believed to be essential in some biological processes (for instance, in the regulation of oncogene transcription) and can be targeted as promising antitumor therapies (*3*−*13*).

Some aptamers (artificial nucleic acid ligands) are known to have G-quadruplex motifs. One of them, PS2.M, when complexed with hemin, has been reported to possess high peroxidase activity (*14*−*16*). Since then, PS2.M has been investigated as a DNAzyme on several occasions (*17*−*21*) and even used as a model to screen G-quadruplex ligands (*22*). Other G-quadruplexes, thrombin binding aptamer (TA, 15-mer) (*23*), AGRO 100 (*24*, *25*), and human telomere (HT) (*22*), have also been shown to possess weak peroxidase activity. We recently observed that, besides PS2.M, some G-quadruplex-forming sequences in gene promoters also formed complexes with hemin and displayed high peroxidase activity, which made us think about whether all G-quadruplex−hemin complexes exhibit peroxidase activity and what types of G-quadruplex−hemin complexes possess high peroxidase activity.

Hemin, the oxidized form of heme released from hemoglobin during several pathological states, has been reported to cause undesirable toxicity leading to organ, tissue, and cellular injury by promoting the formation of oxygen radicals that act as a catalyst in the oxidation of lipids, proteins, and DNA (*26*−*29*). Additionally, oxidative damage to PS2.M in the reaction of the PS2.M−hemin complex and H_2O_2 has been reported (*30*). Thus, if the general peroxidase activity of G-quadruplex−hemin complexes is confirmed, it may imply a potential mechanism for hemin-mediated cellular injury.

In this work, we have investigated the peroxidase activity of different kinds of G-quadruplex structures and discussed the relationship between peroxidase activity and G-quadruplex structures. The application of the peroxidase activity of G-quadruplex−hemin complexes in screening of G-quadruplex ligands has also been demonstrated.

MATERIALS AND METHODS

Instrumentation and Reagents. All DNA sequences (Table 1) were synthesized and purified by Sunbiotech Co. Ltd. (Beijing, China). They were dissolved in Tris-HCl buffer (25 mM, pH 7.6) containing 150 mM NaCl, 20 mM KCl, 0.03% Triton X-100, and 1% DMSO, heated to 95 °C for 5 min, cooled quickly on ice, and then stored at 4 °C. All DNA stock solutions were 20 μM. Hemin was obtained from Beijing XinJingKe Biotechnology Ltd. (Beijing, China). A hemin stock solution (10 mM) was prepared in DMSO and stored in the dark at −20 °C. ABTS was purchased from Amresco. Ethidium bromide (EB) and luminol were from Sigma. H_2O_2 (30%) and other reagents were

[†]This work was supported by the National Science Foundation of China (20775082 and 90717119), the 973 Program (2007CB935601), and the 863 Program (2008AA02Z206).

*To whom correspondence should be addressed. Telephone and fax: (+86) 10-62528509. E-mail: sgdh@iccas.ac.cn.

[1]Abbreviations: c-Myc, human c-myc gene; VEGF, vascular endothelial growth factor; c-Kit21, c-kit gene promoter; HIF-1α, hypoxia inducible factor 1α promoter; RET, RET oncogene promoter; Bcl-2, B-cell CLL/lymphoma 2 gene promoter; HT, human telomeres; TA, thrombin aptamer; CD, circular dichroism; $ABTS^{2-}$, 2,2′-azinobis(3-ethylbenzothiozoline)-6-sulfonic acid; EB, ethidium bromide; NMR, nuclear magnetic resonance; MS, mass spectrometry; TRAP, telomeric repeat amplification protocol; DMSO, dimethyl sulfoxide.

© 2009 American Chemical Society
Published on Web 07/20/2009

Table 1: Kinetic Parameters for (Per)oxidation of ABTS Catalyzed by G-Quadruplex−Hemin Complexes

name	sequence (5′ to 3′)	k_{cat} (s^{-1})	k_c/k_u[a]	G-quadruplex structure	description
G6	$T_4G_6T_4$	0.245 ± 0.024	5.4 ± 0.5	intermolecular parallel	(*34*)
G8	$T_4G_8T_4$	0.312 ± 0.030	6.9 ± 0.7	intermolecular parallel	(*34*)
TA	$G_2T_2G_2TGTG_2T_2G_2$	0.045 ± 0.009	1.0 ± 0.2	intramolecular antiparallel	thrombin aptamer (*46*)
TA2	$G_4T_2G_4TGTG_4T_2G_4$	0.143 ± 0.013	3.2 ± 0.3	intramolecular antiparallel	(*47*)
HT	$AG_3(TTAG_3)_3$	0.105 ± 0.011	2.3 ± 0.2	intramolecular antiparallel	human telomere (*13*)
Oxy28	$G_4T_4G_4T_4G_4T_4G_4$	0.287 ± 0.030	6.4 ± 0.7	intramolecular antiparallel	*Oxytrichia* telomeric (*13*)
Bcl-2	$G_3CGCG_3AG_2A_2G_5CG_3$	0.625 ± 0.060	14 ± 1	coexisting or mixed type hybrid	B-cell CLL/lymphoma 2 (*12*)
PS2.M	$GTG_3TAG_3CG_3T_2G_2$	1.11 ± 0.011	25 ± 0.2	coexisting or mixed type hybrid	hemin aptamer (*15*)
EA2	$CGAGG(TG_3)_3A$	2.29 ± 0.22	51 ± 5	intramolecular parallel	designed sequence
EAD	$C(TG_3)_4A$	3.62 ± 0.28	80 ± 6	intramolecular parallel	designed sequence
EAD2	$CTG_3(AG_3)_3A$	4.28 ± 0.24	95 ± 5	intramolecular parallel	designed sequence
EAD3	$CTG_3(CG_3)_3A$	2.97 ± 0.30	66 ± 7	intramolecular parallel	designed sequence
EAD4	$CTG_3(TTG_3)_3A$	2.85 ± 0.15	63 ± 3	coexisting or mixed type hybrid	designed sequence
EAD6	$C\ (TG_4)_4A$	2.78 ± 0.14	62 ± 3	intramolecular parallel	designed sequence
VEGF	$(G_3C)_2CG_5CG_3$	2.96 ± 0.22	66 ± 5	intramolecular parallel	vascular endothelial growth factor (*8*)
c-Myc	$TGAG_3TG_4AG_3TG_4A_2$	4.18 ± 0.22	93 ± 5	intramolecular parallel	human c-myc gene (*7*)
c-Kit21	$(CG_3)_2(CG)_2(AG_3)_2G$	1.18 ± 0.12	26 ± 3	intramolecular parallel	c-kit gene promoter (*9*)
HIF-1α	$(G_3A)_2GAG_5CG_3$	1.24 ± 0.047	28 ± 1	intramolecular parallel	hypoxia inducible factor 1α (*10*)
RET	$(G_3C)_2G(CG_3)_2$	1.75 ± 0.17	39 ± 4	intramolecular parallel	RET oncogene (*11*)

[a] k_c/k_u equals k_{cat}/k_{uncat}. k_{cat} values were obtained from the equation $k_{cat} = V_{max}/[E]$, and k_{uncat} was the "blank" (hemin) catalytic constant. All the kinetic measurements were repeated at least three times and were found to agree within ±5−10%.

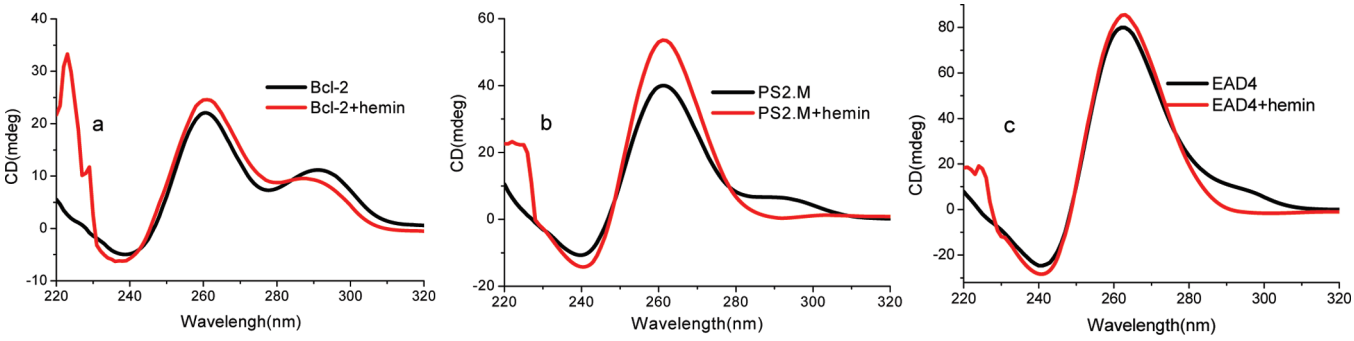

FIGURE 1: CD spectra of G-quadruplexes and G-quadruplex−hemin complexes [concentration ratio of 2:1, at certain DNA concentrations (4−10 μM)].

purchased from Beijing Chemical Plant (Beijing, China). The perylene derivative Tel01 (yield of 86%) was synthesized according to recent reports (*31*, *32*). Tel01 product was confirmed by MALDI-TOF [calcd for $C_{34}H_{32}O_4N_4$ *m*/*z* 560.24, found for Tel01 *m*/*z* 559.8 $[M - H]^-$]: ^1H NMR (1:1 D_2O/CD_3COOD, 400 MHz, 25 °C) δ 7.78 (d, 4H), 7.50 (s, 4H), 4.14 (s, 4H), 3.38 (m, 4H), 3.05 (m, 12H), 1.91 (s, 4H). All solutions were prepared with deionized water purified by a Milli-Q system (Millipore). Hemin, luminol, ABTS, and H_2O_2 working solutions were freshly prepared with Tris-HCl buffer (25 mM, pH 7.6) containing 150 mM NaCl, 20 mM KCl, 0.03% Triton X-100, and 1% DMSO before being used.

Catalytic Kinetics Experiments. Using SpectraMax M5 (Molecular Devices) at room temperature, kinetics were followed by monitoring the appearance of the radical anion ($ABTS^{\bullet-}$) at 414 nm over 3 min for peroxidations catalyzed by either G-quadruplex−hemin (concentration ratio of 2:1) complexes or hemin alone (blank experiments, without G-quadruplex). All kinetic experiments were conducted in microplates containing buffer, hemin (or G-quadruplex−hemin complex), and ABTS. Reactions were initiated by the addition of H_2O_2. Increases in absorbance at 414 nm were measured as a function of time. The initial rates were calculated from the slope of the initial linear portion (usually the first 20 s) of the increase in absorbance. All kinetic measurements were repeated at least three times and were found to agree within ±5−10%. The Δε value used was 36000 M^{-1} cm^{-1} (*15*). Kinetic parameters (K_m and V_{max}) of the peroxidase-catalyzed reactions were obtained using the Michaelis equation.

CD Spectra. CD spectra (220−320 nm) were recorded on a Jasco J-815 circular dichroism spectropolarimeter (JASCO Ltd.) at a rate of 500 nm/min using 400 μL of 1 cm fused quartz cells. Measurements were taken in 25 mM Tris-HCl (pH 7.6) containing 150 mM NaCl, 20 mM KCl, DNA at certain concentrations (4−10 μM), and the DNA−hemin (concentration ratio of 2:1) complex at room temperature. To facilitate comparisons, the CD spectra were background subtracted, smoothed, and calibrated for concentration so that molar ellipticities could be obtained.

Thermal Denaturation. UV and CD melting curves of G-quadruplexes or G-quadruplex−hemin (concentration ratio of 1:1) complexes in the absence and presence of K^+ were monitored at 295 nm for absorbance and 260 nm for CD signals using a Jasco J-815 circular dichroism spectropolarimeter (JASCO Ltd.). The samples were heated from 5 to 95 °C at a rate of 2 °C/min. Before measurement, all the samples were heated at 95 °C for 5 min, cooled quickly on ice, and then stored at 4 °C overnight.

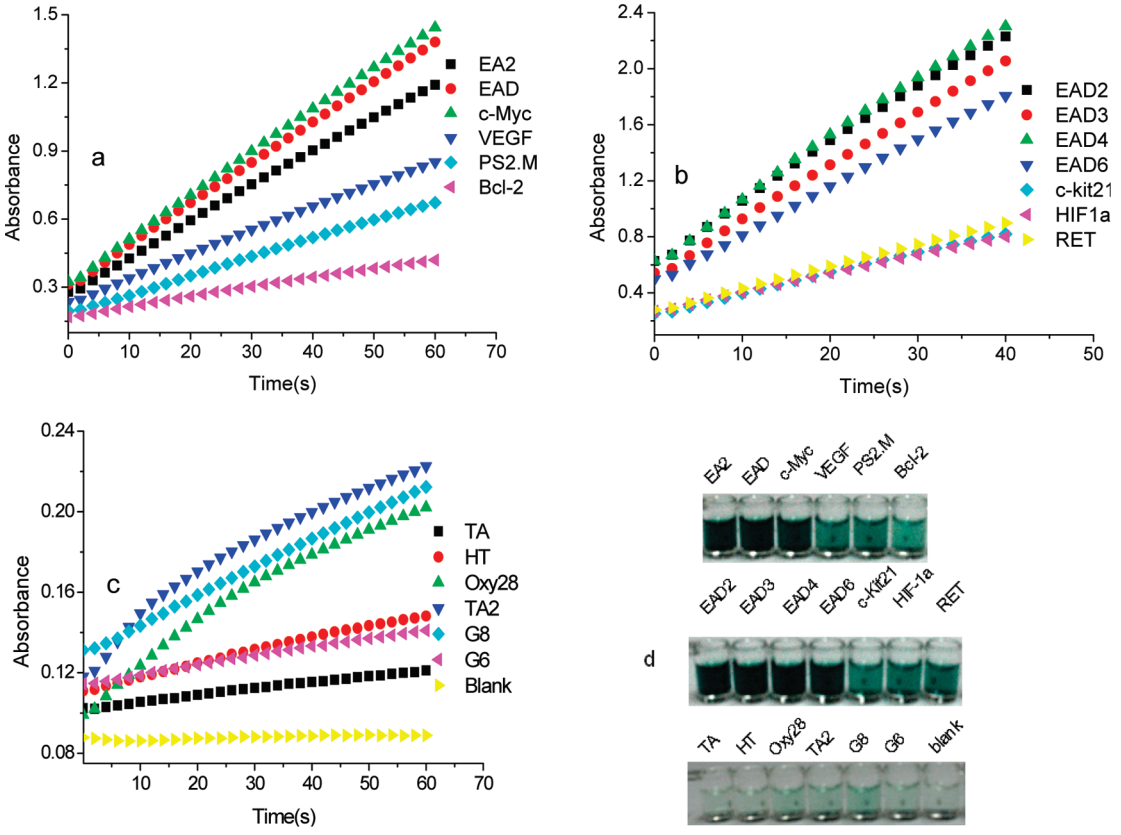

FIGURE 2: Peroxidase activity of G-quadruplex−hemin complexes. (a−c) Catalytic kinetics of each G-quadruplex−hemin complex within 60 s (absorbance change at 414 nm). (d) Photographs of oxidation of ABTS by H_2O_2 in the presence of G-quadruplex−hemin complexes. Photographs were taken 5 min after mixing. Twenty microliters of different G-quadruplexes at 20 μM and 20 μL of 10 μM hemin were mixed at room temperature for 2 h, and then ABTS and H_2O_2 were added until the volume reached 200 μL. The final concentrations were as follows: 2 μM G-quadruplexes, 1 μM hemin, 2 mM ABTS, and 2 mM H_2O_2. Each well or curve is marked with the corresponding G-quadruplex name.

Table 2: Effect of K^+ on G-Quadruplex−Hemin Peroxidase Activity[a]

G-quadruplex	V_{obs} (nM s^{-1}) without K^+	V_{obs} (nM s^{-1}) with 20 mM K^+
blank	2.17	7.50
G6	10.8	46.7
G8	19.5	73.3
TA	7.17	13.0
HT	10.3	26.2
PS2.M	30.2	205
c-Myc	23.2	465
VEGF	15.7	327
Bcl-2	15.8	116
EA2	28.8	340
EAD	29.0	452

[a] Twenty microliters of 10 μM hemin and 20 μL of different G-quadruplexes at 20 μM were incubated at room temperature for at least 2 h, and then ABTS and H_2O_2 were added until the volume reached 200 μL to give a final concentration of 2 mM for both. V_{obs} values were calculated from the slope of the initial linear portion of the increase in absorbance.

Table 3: T_m Values (±1 °C) of G-Quadruplexes or G-Quadruplex−Hemin Complexes in the Absence and Presence of K^+ or Hemin[a]

G-quadruplex	K^+(−)	K^+(+)	K^+(−),hemin(+)	K^+(+),hemin(+)
EA2	31	44	41	68
EAD	43	>80	47	78
VEGF	48	>80	45	64
c-Myc	43	79	41	77

[a] Legend: K^+(−), buffer without K^+; K^+(+), buffer containing 20 mM K^+; K^+(−),hemin(+), buffer without K^+ but containing hemin [concentration ratio of 1:1, with a certain DNA concentration (4−10 μM)]; K^+(+),hemin(+), buffer containing 20 mM K^+ containing hemin [concentration ratio of 1:1, with a certain DNA concentration (4−10 μM)].

RESULTS AND DISCUSSION

To reveal the connection between peroxidase activity and G-quadruplexes, we have investigated many different G-quadruplex structures found in human gene promoters (c-Myc, VEGF, RET, HIF-1α, c-Kit21, and Bcl-2), human telomeres (HT), and thrombin aptamer (TA), including parallel, antiparallel, and mixed antiparallel/parallel G-quadruplex structures (Table 1). It is well-known that G-quadruplexes exhibit characteristic CD signals depending on their strand composition. Antiparallel G-quadruplexes have a CD spectrum characterized by a positive ellipticity maximum around 295 nm and a negative minimum around 260 nm, while parallel quadruplexes have a positive maximum around 264 nm and a negative minimum around 240 nm. CD spectra with peaks at both 264 and 295 nm could indicate either the coexistence of distinct parallel and antiparallel folded species in solution or a single mixed-type hybrid quadruplex structure (*33*). The structure determination of all quadruplexes in this report under the experimental conditions was confirmed by CD spectra (Figure 1 and Figure S1 of the Supporting Information).

The peroxidase activities were measured on the basis of the (per)oxidation of $ABTS^{2-}$ in the presence of hydrogen peroxide to produce the colored radical anion ($ABTS^{\bullet-}$). As shown in

Figure 2 and Table 1, different types of G-quadruplex structures exhibit different peroxidase activities: all intramolecular parallel structures investigated here possess strong peroxidase activities, most of which (such as those of c-Myc, VEGF, EAD, EAD2, EAD3, and RET) are much higher than that of the widely used DNAzyme, PS2.M, while the intramolecular antiparallel G-quadruplex structures (as in TA, TA2, HT, and Oxy28) have only very weak activities. The coexisting or mixed-type hybrid parallel and antiparallel structures (as in Bcl-2, PS2.M, and EAD4) also exhibit strong peroxidase activities, and the sequences with a higher ratio of parallel to antiparallel structures (ratio of the CD peak at 260 nm to that at 295 nm) exhibit higher peroxidase activity (Figures 1 and 2 and Table 1). In addition, the intermolecular parallel-stranded G-quadruplexes (G6 and G8) (*34*) show only very weak peroxidase activity. All peroxidase activities were also confirmed with a chemiluminescent assay based on peroxidation of luminol in the presence of hydrogen peroxide (data not shown). These results indicate that G-quadruplex−hemin complexes possess general peroxidase activity. The intramolecular parallel G-quadruplex structures may be essential for catalysis.

Scheme 1: Proposed Structural Models for (A) the Intramolecular Parallel Quadruplex−Hemin Complex, (B) the Intramolecular Antiparallel Quadruplex−Hemin Complex, and (C) the Intermolecular Parallel Quadruplex−Hemin Complex

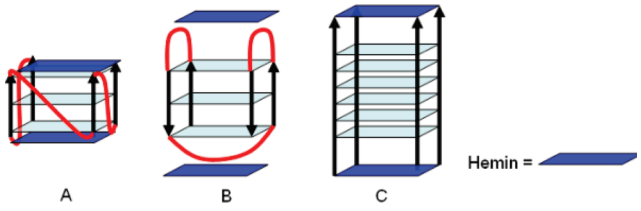

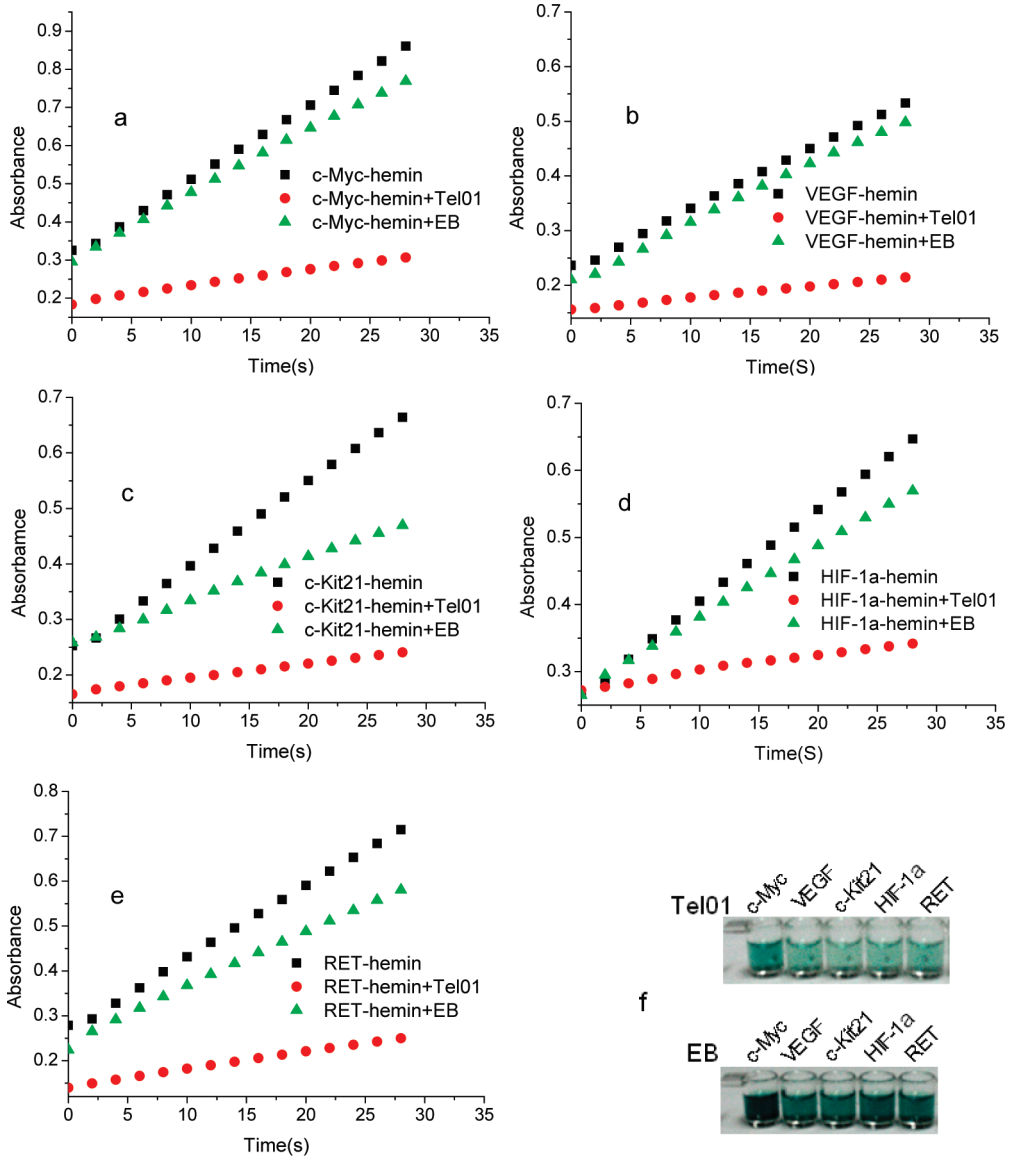

FIGURE 3: Inhibiting ability of Tel01 or EB on the peroxidase activity of G-quadruplex−hemin complexes. (a−e) Catalytic kinetics of each G-quadruplex−hemin complex within 60 s (absorbance change at 414 nm): (a) c-Myc, (b) VEGF, (c) c-Kit21, (d) HIF-1α, and (e) RET gen promoters. (f) Photographs of the oxidation of ABTS by H_2O_2 in the presence of G-quadruplex−hemin complexes. For Tel01 (top) and EB (bottom), photographs were taken 5 min after mixing; each well is marked with the corresponding G-quadruplex name. Twenty microliters of different G-quadruplexes at 20 μM, 10 μL of 20 μM hemin, and 10 μL of 20 μM Tel01 or EB were mixed at room temperature for 2 h, and then ABTS and H_2O_2 were added until the volume reached 200 μL. The final concentrations were as follows: 2 μM G-quadruplexes, 1 μM hemin, 1 μM Tel01 or EB, 2 mM ABTS, and 2 mM H_2O_2.

K^+ is well-known to play an important role in the formation and stabilization of G-quadruplex structures, or even alter the conformations of G-quadruplexes (*35*). Therefore, the influence of K^+ on the peroxidase activity was investigated. As shown in Table 2, the catalytic rates in the absence of K^+ are found to be much lower than those in the presence of 20 mM K^+. The thermal denaturation assay also showed a much lower melting temperature (T_m) of G-quadruplex structures in the absence of K^+ than in the presence of K^+ (Table 3). These two sets of results indicate that stable G-quadruplex structure is essential for peroxidase activity. The additions of hemin to G-quadruplex solutions did not have a significant influence on the CD spectra of the parallel and antiparallel G-quadruplex structures (Figure S1 of the Supporting Information) except for slightly decreasing the magnitudes of the 295 nm peaks and increasing those of the 264 nm peaks (Figure 1) of the mixed antiparallel/parallel sequences (Bcl-2, PS2.M, and EAD4) under our conditions. However, additions of hemin changed the T_m values of some intramolecular parallel G-quadruplexes (Table 3). These results suggest that the interaction of hemin with G-quadruplexes influences their thermal stability but may not alter the conformation of the G-quadruplex structures.

Intramolecular G-quadruplex formation requires three loops to link the G-tetrads. For the parallel structure, the loops adopt a propeller-type form (*36*) to link two adjacent parallel strands from the top to the bottom G-tetrads; namely, loops distribute on the side faces of the G-quadruplex. For the antiparallel structure, loops bridge either two diagonally opposite (diagonal loops) or two adjacent (edgewise loops) antiparallel strands (*33*); namely, loops distribute on the top and bottom surfaces. Many small-molecule ligands have been proposed to interact with G-quadruplexes on their ends by end stacking (*34*, *37*). Additionally, the peroxidative activity of the PS2.M−hemin complex has been suggested to be a result of the interaction of specific guanines of PS2.M with the bound hemin cofactor (*30*). Clearly, the parallel structure is in favor of the end stacking of ligands, including hemin, which could explain the high peroxidase activity of parallel G-quadruplex−hemin complexes (Scheme 1). The difference in catalytic activities among the parallel G-quadruplexes might be due to small steric hindrances caused by their different loop structures. On the other hand, antiparallel G-quadruplex−hemin complexes had weak peroxidase activity, which might be caused by the large steric hindrance of the loops which obstructed the interaction of specific guanines in G-quadruplexes with the bound hemin cofactor. For the intermolecular parallel-stranded G-quadruplexes, G6 and G8, their T4 termini at the two ends of the G-quadruplexes also hinder the end stacking of hemin, leading to weak peroxidase activities. Since hemin and heme (reduced state of hemin) are complexes of iron with protoporphyrin IX that serve as the prosthetic group of numerous hemoproteins (e.g., hemoglobin, myoglobin, cytochromes, guanylate cyclase, and nitric oxide synthase) and play an important role in controlling protein synthesis and cell differentiation (*38*, *39*), this general peroxidase activity of G-quadruplex−hemin complexes may suggest a previously unknown biological role of G-quadruplexes in cellular functions. Additionally, oxidative damage to PS2.M in the reaction of the PS2.M−hemin complex and H_2O_2 has been reported (*30*). Hemin has been found to have a cytotoxic effect by promoting the formation of oxygen radicals that act as a catalyst in the oxidation of lipids, proteins, and DNA (*26*−*29*); therefore, the general peroxidase activity of G-quadruplex−hemin complexes may also imply a new mechanism of cellular injury.

Table 4: Catalytic Constants of Oxidation of ABTS by H_2O_2 in the Presence of Hemin, Parallel G-Quadruplex Sequences in Gene Promoters, and Tel01 or EB[a]

G-quadruplex−hemin complex	$k_{cat,Tel01}$ (s^{-1})	$k_{cat,EB}$ (s^{-1})
c-Myc−hemin	1.32 ± 0.243	3.22 ± 0.14
VEGF−hemin	0.475 ± 0.057	1.51 ± 0.167
c-Kit-21−hemin	0.528 ± 0.087	0.940 ± 0.022
HIF-1α−hemin	0.225 ± 0.017	1.22 ± 0.032
RET−hemin	0.372 ± 0.090	1.24 ± 0.047

[a] Twenty microliters of different G-quadruplexes at 20 μM, 10 μL of 20 μM hemin, and 10 μL of 20 μM Tel01 or EB were incubated at room temperature for at least 2 h, and then ABTS and H_2O_2 were added until the volume reached 200 μL to give a final concentration of 2 mM for both.

We next explored the application of the peroxidase activity of G-quadruplex−hemin complexes in studying G-quadruplex−ligand interactions. Despite the fact that G-quadruplex-forming sequences occur throughout the genomes of most organisms, their exact functions are not yet well understood. The search for small-molecule ligands that can interact with specific G-quadruplexes and regulate their biological activities is a challenge with major implications for both fundamental studies and drug discovery. For example, some organic molecules that recognize G-quadruplexes have been demonstrated to inhibit telomerase, an enzyme that is crucial for sustaining many cancer cells and thus an important target for cancer therapy (*40*, *41*). The techniques for studying ligands of G-quadruplexes include NMR (*42*, *43*), MS (*31*, *44*), telomeric repeat amplification protocol (TRAP) assays (*45*), etc. Though these methods can give definitive evidence of the interactions of G-quadruplexes with ligands, when applied for ligand screening, they are time-consuming and, expensive and often rely on complex instruments. Herein, we describe a high-throughput method for screening active G-quadruplex ligands on the basis of the high peroxidase activity of G-quadruplex−hemin complexes. Ligands competing with hemin for binding to G-quadruplexes can reduce the colored product generated by the (per)oxidation of $ABTS^{2-}$. Consequently, the G-quadruplex binding capability of the given ligands can be monitored by "the naked eye" at room temperature according to the decrease in the color intensity.

In our experiment, intramolecular parallel G-quadruplex-forming sequences on important human gene promoters (c-Myc, VEGF, c-Kit21, HIF-1α, and RET) were used as model targets, a positively charged end stacking G-quadruplex binder with a large π-aromatic surface, perylene derivative Tel01 (*2*, *31*, *32*), was used as a model positive ligand, and a typical duplex binder ethidium bromide (EB) was used as a model negative control. As shown in Figure 3, positive agent Tel01 strongly competed against hemin and greatly reduced the deep color of radical anion ($ABTS^{\bullet -}$) compared to the negative control EB. The catalytic rates of G-quadruplex−hemin complexes in the presence of Tel01 decreased by 44−82% (Table 4) compared to that in the presence of EB. The inhibiting abilities of different G-quadruplex−hemin complexes are different. These results demonstrate that the proposed method can be used as a primary technique for high-throughput screening of potential ligands (potential anticancer reagents) for specific G-quadruplex sequences using colorimetric and visual detection strategies. Compared to using PS2.M as a model sequence to screen G-quadruplex ligands (*22*), using the specific G-quadruplex sequences would have better specificity and accuracy since

our results have demonstrated the different responses of the same ligand (such as hemin and Tel01) to different G-quadruplexes.

CONCLUSION

In conclusion, we have shown the general peroxidase activity of G-quadruplex−hemin complexes. The intramolecular parallel G-quadruplex structure favors the end stacking of hemin, therefore possessing high peroxidase activity. This peroxidase activity of the hemin complexed with G-quadruplex-forming sequences in gene promoters may imply a potential mechanism of hemin-mediated cellular injury. The structure-dependent peroxidase activity has also been demonstrated to be applicable for colorimetric screening of G-quadruplex ligands.

SUPPORTING INFORMATION AVAILABLE

CD spectra of G-quadruplexes and their G-quadruplex−hemin complexes (Figure S1). This material is available free of charge via the Internet at http://pubs.acs.org.

REFERENCES

1. Burge, S., Parkinnson, G. N., Hazel, P., Todd, A. K., and Neidle, S. (2006) Survey and summary quadruplex DNA: Sequence, topology and structure. *Nucleic Acids Res. 34*, 5402–5415.
2. Davis, J. (2004) G-quartets 40 years later: From 5′-GMP to molecular biology and supramolecular chemistry. *Angew. Chem. 116*, 684–716; *Angew. Chem., Int. Ed. 43*, 668−698.
3. Todd, A. K., Johnston, M., and Neidle, S. (2005) Highly prevalent putative quadruplex sequence motifs in human DNA. *Nucleic Acids Res. 33*, 2901–2907.
4. Huppert, J. L., and Balasubramanian, S. (2005) Prevalence of quadruplexes in the human genome. *Nucleic Acids Res. 33*, 2908–2916.
5. Huppert, J. L., and Balasubramaniam, S. (2007) G-quadruplexes in promoters throughout the human genome. *Nucleic Acids Res. 35*, 406–413.
6. Eddy, J., and Maizels, N. (2006) Gene function correlates with potential for G4 DNA formation in the human genome. *Nucleic Acids Res. 34*, 3887–3896.
7. Phan, A. T., Modi, Y. S., and Patel, D. J. (2004) Propeller-type parallel-stranded G-quadruplexes in the human c-myc promoter. *J. Am. Chem. Soc. 126*, 8710–8716.
8. Sun, D., Guo, K., Rusche, J. J., and Hurley, L. H. (2005) Facilitation of a structural transition in the polypurine/polypyrimidine tract within the proximal promoter region of the human VEGF gene by the presence of potassium and G-quadruplex-interactive agents. *Nucleic Acids Res. 33*, 6070–6080.
9. Fernando, H., Reszka, A. P., Huppert, J., Ladame, S., Rankin, S., Venkitaraman, A. R., Neidle, S., and Balasubramanian, S. (2006) A conserved quadruplex motif located in a transcription activation site of the human c-kit oncogene. *Biochemistry 45*, 7854–7860.
10. Armond, R. D., Wood, S., Sun, D., Hurley, L. H., and Ebbinghaus, S. W. (2005) Evidence for the presence of a guanine quadruplex forming region within a polypurine tract of the hypoxia inducible factor 1α promoter. *Biochemistry 44*, 16341–16350.
11. Guo, K., Pourpak, A., Beetz-Rogers, K., Gokhale, V., Sun, D., and Hurley, L. H. (2007) Formation of pseudosymmetrical G-quadruplex and i-motif structures in the proximal promoter region of the RET oncogene. *J. Am. Chem. Soc. 129*, 10220–10228.
12. Dai, J., Chen, D., Jones, R. A., Hurley, L. H., and Yang, D. (2006) NMR solution structure of the major G-quadruplex structure formed in the human BCL2 promoter region. *Nucleic Acids Res. 34*, 5133–5144.
13. Zhou, J., Yuan, G., Liu, J., and Zhan, C. G. (2007) Formation and stability of G-quadruplexes self-assembled from guanine-rich strands. *Chem.—Eur. J. 13*, 945–949.
14. Li, Y., and Sen, D. (1997) Toward an efficient DNAzyme. *Biochemistry 36*, 5589–5599.
15. Travascio, P., Li, Y., and Sen, D. (1998) DNA-enhanced peroxidase activity of a DNA aptamer-hemin complex. *Chem. Biol. 5*, 505–517.
16. Li, Y., Geyer, R., and Sen, D. (1996) Recognition of anionic porphyrins by DNA aptamers. *Biochemistry 35*, 6911–6922.
17. Li, T., Li, B., and Dong, S. (2007) Aptamer-based label-free method for hemin recognition and DNA assay by capillary electrophoresis with chemiluminescence detection. *Anal. Bioanal. Chem. 389*, 887–893.
18. Li, D., Shlyahovsky, B., Elbaz, J., and Willner, I. (2007) Amplified analysis of low-molecular-weight substrates or proteins by the self-assembly of DNAzyme-aptamer conjugates. *J. Am. Chem. Soc. 129*, 5804–5805.
19. Xiao, Y., Pavlov, V., Niazov, T., Dishon, A., Kotler, M., and Willner, I. (2004) Catalytic beacons for the detection of DNA and telomerase activity. *J. Am. Chem. Soc. 126*, 7430–7431.
20. Deng, M., Zhang, D., Zhou, Y., and Zhou, X. (2008) Highly effective colorimetric and visual detection of nucleic acids using an asymmetrically split peroxidase DNAzyme. *J. Am. Chem. Soc. 130*, 13095–13102.
21. Lu, N., Shao, C., and Deng, Z. (2008) Rational design of an optical adenosine sensor by conjugating a DNA aptamer with split DNAzyme halves. *Chem. Commun.,* 6161–6163.
22. Kong, D. M., Wu, J., Ma, Y. E., and Shen, H. X. (2008) A new method for the study of G-quadruplex ligands. *Analyst 133*, 1158–1160.
23. Li, T., Wang, E., and Dong, S. (2008) G-quadruplex-based DNAzyme for facile colorimetric detection of thrombin. *Chem. Commun.,* 3654–3656.
24. Li, T., Dong, S., and Wang, E. (2009) Label-free colorimetric detection of aqueous mercury ion (Hg^{2+}) using Hg^{2+}-modulated G-quadruplex-based DNAzymes. *Anal. Chem. 81*, 2144–2149.
25. Li, T., Wang, E., and Dong, S. (2009) G-quadruplex-based DNAzyme as a sensing platform for ultrasensitive colorimetric potassium detection. *Chem. Commun.,* 580–582.
26. Kumar, S., and Bandyopadhyay, U. (2005) Free heme toxicity and its detoxification systems in human. *Toxicol. Lett. 157*, 175–188.
27. Regan, R. F., Kumar, N., Gao, F., and Guo, Y. (2002) Ferritin induction protects cortical astrocytes from heme-mediated oxidative injury. *Neuroscience 113*, 985–994.
28. Chen-Roetling, J., Benvenisti-Zarom, L., and Regan, R. F. (2005) Cultured astrocytes from heme oxygenase-1 knockout mice are more vulnerable to heme-mediated oxidative injury. *J. Neurosci. Res. 82*, 802–810.
29. Aft, R. L., and Mueller, G. C. (1983) Hemin-mediated DNA strand scission. *J. Biol. Chem. 258*, 12069–12072.
30. Travascio, P., Witting, P., Mauk, A., and Sen, D. (2001) The peroxidase activity of a hemin-DNA oligonucleotide complex: Free radical damage to specific guanine bases of the DNA. *J. Am. Chem. Soc. 123*, 1337–1348.
31. Zhou, J., and Yuan, G. (2007) Specific recognition of human telomeric G-quadruplex DNA with small molecules and the conformational analysis by ESI mass spectrometry and circular dichroism spectropolarimetry. *Chem.—Eur. J. 13*, 5018–5023.
32. Kern, J. T., Thomas, P. W., and Kerwin, S. M. (2002) The relationship between ligand aggregation and G-quadruplex DNA selectivity in a series of 3,4,9,10-perylenetetracarboxylic acid diimides. *Biochemistry 41*, 11379–11389.
33. Bugaut, A., and Balasubramanian, S. (2008) A sequence-independent study of the influence of short loop lengths on the stability and topology of intramolecular DNA G-quadruplexes. *Biochemistry 47*, 689–697.
34. Evans, S. E., Mendez, M. A., Turner, K. B., Keating, L. R., Grimes, R. T., Melchoir, S., and Szalai, V. A. (2007) End-stacking of copper cationic porphyrins on parallel-stranded guanine quadruplexes. *J. Biol. Inorg. Chem. 12*, 1235–1249.
35. Ambrus, A., Chen, D., Dai, J., Bialis, T., Jones, R. A., and Yang, D. (2006) Human telomeric sequence forms a hybrid-type intramolecular G-quadruplex structure with mixed parallel/antiparallel strands in potassium solution. *Nucleic Acids Res. 34*, 2723–2735.
36. Hazel, P., Huppert, J., Balasubramanian, S., and Neidle, S. (2004) Loop-length-dependent folding of G-quadruplexes. *J. Am. Chem. Soc. 126*, 16405–16415.
37. Gavathiotis, E., Heald, R. A., Stevens, M. F. G., and Searle, M. S. (2001) Recognition and stabilization of quadruplex DNA by a potent new telomerase inhibitor: NMR studies of the 2:1 complex of a pentacyclic methylacridinium cation with $d(TTAGGGT)_4$. *Angew. Chem. 113*, 4885–4887; *Angew. Chem., Int. Ed. 40*, 4749−4751.
38. Bowman, S. E. J., and Bren, K. L. (2008) The chemistry and biochemistry of heme c: Functional bases for covalent attachment. *Nat. Prod. Rep. 25*, 1118–1130.
39. Ponka, P. (1999) Cell biology of heme. *Am. J. Med. Sci. 318*, 241–256.
40. Oganesian, L., and Bryan, T. M. (2007) Physiological relevance of telomeric G-quadruplex formation: A potential drug target. *BioEssays 29*, 155–165.

41. Neidle, S., and Read, M. A. (2001) G-quadruplexes as therapeutic targets. *Biopolymers 56*, 195–208.
42. Zhou, Q., Li, L., Xiang, J., Tang, Y., Zhang, H., Yang, S., Li, Q., Yang, Q., and Xu, G. (2008) Screening potential antitumor agents from natural plant extracts by G-quadruplex recognition and NMR methods. *Angew. Chem. 120*, 5672–5674; *Angew. Chem., Int. Ed. 47*, 5590−5592.
43. Fedoroff, O. Y., Salazar, M., Han, H., Chemeris, V. V., Kerwin, S. M., and Hurley, L. H. (1998) NMR-based model of a telomerase-inhibiting compound bound to G-quadruplex DNA. *Biochemistry 37*, 12367–12374.
44. Rosu, F., Pauw, E. D., Guittat, L., Alberti, P., Lacroix, L., Mailliet, P., Riou, J. F., and Mergny, J. L. (2003) Selective interaction of ethidium derivatives with quadruplexes: An equilibrium dialysis and electrospray ionization mass spectrometry analysis. *Biochemistry 42*, 10361–10371.
45. Gomez, D., Mergny, J. L., and Riou, J. F. (2002) Detection of telomerase inhibitors based on G-quadruplex ligands by a modified telomeric repeat amplification protocol assay. *Cancer Res. 62*, 3365–3368.
46. Macaya, R. F., Schultze, P., Smith, F. W., Roe, J. A., and Feigon, J. (1993) Thrombin-binding DNA aptamer forms a unimolecular quadruplex structure in solution. *Proc. Natl. Acad. Sci. U.S.A. 90*, 3745–3749.
47. Rehder, M., and McGown, L. (2001) Open-tubular capillary electrochromatography of bovine β-actoglobulin variants A and B using an aptamer stationary phase. *Electrophoresis 22*, 3759–3764.